Proceedings of the 1999 IEEE
International Conference on Robotics & Automation
Detroit, Michigan • May 1999

Intelligent Compliance Control for Robot Manipulators Using Adaptive Stiffness Characteristics

Byoung-Ho Kim[†, ‡], Nak Young Chong[°], Sang-Rok Oh[†], Il Hong Suh[‡], and Young-Jo, Cho[†]

† : Intelligent System Control Research Center, KIST, Seoul, Korea
(E-mail: sroh@amadeus.kist.re.kr)
o : Biorobotics Div., Robotics Dept., MEL, Japan (Email: chong@mel.go.jp)
‡ : Intelligent Control and Robotics Lab., Hanyang Univ., Seoul, Korea
(E-mail: ihsuh@email.hanyang.ac.kr)

Abstract

A compliance control strategy for robot manipulators is proposed in this paper by employing a self-adjusting stiffness function. To be specific, each entry of the diagonal stiffness matrix corresponding to task coordinate in Cartesian space is adaptively adjusted during contact along the corresponding axis based on the contact force with its environment. And also, it can be used for both unconstrained and constrained motions without any switching mechanism which often causes undesirable instability and/or vibrational motion of the end-effector. The experimental results show the effectiveness of the proposed method by employing a two-link direct drive manipulator interacting with an unknown environment.

1 Introduction

When a robot manipulator is applied in real environments such as doing service tasks as well as industrial automation, many manipulation tasks often require a series of contact operations. A contact motion is typically obtained by phase transition from an unconstrained motion to a constrained motion. However, if contact failed to be maintained after impact, there is a possible bouncing for phase transitions partly because if the method employs algorithmic switching between two motions or high stiffness gain. In fact, a conventional position servo for an industrial robot is designed to be infinitely stiff that is appropriate when the manipulator is applied to follow a given trajectory in a free space, and hence it will reject all force disturbances acting on the system. However, a contact is made between the end-effector and the environment, high stiffness of the end-effector or the environment can make the manipulator be failed to maintain the contact. Small variations in relative positions due to either inaccuracy in position information or errors in position servo can produce undesirable large contact forces. To remedy this problem, force servo instead of position servo may be used, where an ideal force servo exhibits zero stiffness and be able to maintain the desired force. However, force servo cannot be useful for trajectory following due to sensitive positional variation even for a small external force disturbances. One way to alleviate these problems is to use a compliant motion controller: Some axes of the task coordinate are selected to be force controlled, and others position-controlled.

In order to handle the interaction of a robot manipulator with an environment, many researchers have been studied in the field of the compliant motion control of robot manipulators [1]. The well known hybrid position/force control approach [2, 3] is based on an orthogonal decomposition of the task space. In the scheme, however, since the selection matrix should be determined a *priori* according to position controlled or force controlled axis, it can not be appllied for the task interacting with an unknown environment. A position error based stiffness adaptation scheme has been proposed in [4]. However, since the exact trajectory tracking is assumed with high stiffness gain in unconstrained space, a recovery mechanism which resets the stiffness adaptation procedure caused by unexpected position error in unconstrained space should be taken into consideration. In [5], a parallel control scheme with stiffness adaptation has been proposed. The method is useful for regulating contact force in constrained space. But, since it doesn't also have a recovery procedure in the stiffness adaptation algo-

0-7803-5180-0-5/99 $10.00 © 1999 IEEE

rithm, the trajectory tracking performance may not be guaranteed when the task space is changed from constrained space to unconstrained space after performing the constrained task.

In order to handle a contact control problem in an unknown environment, a novel type of compliant contact control method is proposed in this paper. Specifically, the stiffness of the end-effector of a robot manipulator is automatically adjusted based on the contact force with its environment without any switching between constrained and unconstrained space, and hence the method has a stiffness adaptation capability for a successful motion control of the robot manipulator at both constrained and unconstrained space. The proposed algorithm can be effectively applied to cooperative motion control, soft touching and grasping by robot hand.

2 Robot Dynamics and Stiffness Control

When an n degrees-of-freedom robot manipulator contacts its environment, the robot or environment will deform and a reaction force at the end-effector will be transmitted into each joint. If f is a reaction force at the end-effector in Cartesian coordinate, then the dynamic equation takes the form [6],

$$\tau = M(q)\ddot{q} + H(q,\dot{q})\dot{q} + g(q) + J^T(q)f, \qquad (1)$$

where q, $\dot{q}$, and $\ddot{q}$ are $n \times 1$ vectors of joint positions, velocities, and accelerations, respectively. τ is the $n \times 1$ vector of joint torques supplied by the actuator. $M(q)$ is the $n \times n$ symmetric positive definite inertia matrix and $H(q,\dot{q})$ is the $n \times n$ structural matrix of centripetal and Coriolis forces. $g(q)$ is the $n \times 1$ vector of gravity. $J(q)$ is the $n \times n$ Jacobian matrix, relating joint velocities to task space velocities.

From the basic stiffness formulation in the Salisbury's work [7], the joint stiffness matrix K_q is obtained by

$$K_q = J^T K_c J, \qquad (2)$$

where K_c denotes a desired $n \times n$ stiffness matrix in Cartesian space. For stiffness control, the control input is given by [7]

$$\begin{aligned} \tau &= K_q(q_d - q) + K_d(\dot{q}_d - \dot{q}) \\ &\quad + K_f(K_q(q_d - q) - J^T f) + g(q), \end{aligned} \qquad (3)$$

where q_d and $\dot{q}_d$ are $n \times 1$ vectors of desired joint positions and velocities, respectively. K_d is the velocity damping matrix, and K_f is the force feedback gain matrix.

In the Salisbury's work [7], since the method must initially select the desired Cartesian stiffness, it can not be effectively applied for the robot manipulator interacting with an unknown environment. In order to handle this problem, a new compliance control law with adaptive stiffness function is proposed in next section.

3 Compliance Control Law with Adaptive Stiffness Function

3.1 Compliance Control Law

In this paper, the control input for compliant contact control of a robot manipulator is simply given by

$$\tau = K_q(f)(q_d - q) - K_d(f)\dot{q} + g(q), \qquad (4)$$

in joint space, or by using Eq. (2),

$$\tau = J^T(q)(K_c(f)(x_d - x) - K_v(f)\dot{x}) + g(q), \qquad (5)$$

in Cartesian space. In Eq. (5), x, $\dot{x}$, and x_d are the $n \times 1$ position, velocity, and desired position vector in Cartesian space, respectively. $K_c(f)$ and $K_v(f)$ are $n \times n$ diagonal, positive definite stiffness and damping matrix, respectively.

Now, we propose a new nonlinear stiffness adaptation method. For convenient representation, the method can be described in three-dimensional space as follows:

$$K_q(f) = J^T K_c(f) J, \quad K_d(f) = J^T K_v(f) J, \qquad (6)$$

where

$$K_c(f) = \begin{pmatrix} K_{cx}e^{-s_x|f_x|} & 0 & 0 \\ 0 & K_{cy}e^{-s_y|f_y|} & 0 \\ 0 & 0 & K_{cz}e^{-s_z|f_z|} \end{pmatrix}, \qquad (7)$$

and

$$K_v(f) = \begin{pmatrix} \alpha_x & 0 & 0 \\ 0 & \alpha_y & 0 \\ 0 & 0 & \alpha_z \end{pmatrix} K_c(f). \qquad (8)$$

In Eq. (7), K_{cx}, K_{cy}, and K_{cz} represent x, y, and z-directional Cartesian stiffness gain, respectively. Those parameters are chosen to be positive constants with which the asymptotic stability is ensured in unconstrained space. The slope parameters s_x, s_y, and s_z are selected to be positive value and play the role

of determining the decreasing rate. f_x, f_y, and f_z are the directional contact force sensed at the end-effector. In Eq. (8), α_x, α_y, and α_z are positive scalar scaling coefficients.

Several points can be addressed for the proposed method. First, since each entry of the stiffness gain matrix K_c corresponds to the task coordinate in Cartesian space and decreases exponentially during contact only along the corresponding axes, the proposed method has the capability of self-adjusting the stiffness appropriate for the given tasks regardless of constrained and unconstrained space. Second, the method has no switching mechanism which often causes undesired vibrational motions of the end-effector. And hence, the method can be effectively used for both unconstrained and constrained motion control. Third, when the robot manipulator returns to unconstrained space from constrained one, the adjusted stiffness gains are automatically recovered to initially specified stiffness gains K_{cx}, K_{cy}, and K_{cz} in Eq. (7), which is often set to be high enough to guarantee the position tracking performance in unconstrained space. Finally, the method does not require any a *priori* information on the environments, it can be applicable for complicated and even unspecified robotic tasks such as soft touching and grasping by robotic hands.

3.2 Stability Analysis

Now, we have the stability analysis for the robot manipulator interacting with an unknown environment for the proposed stiffness adaptation strategy. The force exerted on the environment is defined as

$$f = K_w(x - x_w), \tag{9}$$

where K_w is $n \times n$ diagonal, positive semi-definite, constant matrix to denote the environmental stiffness, and x_w is an $n \times 1$ vector mesured in task space to denote the static location of the environment and x is the actual position of the end-effector.

Note that if the manipulator is not constrained in a particular task space direction, the corresponding diagonal element of the matrix K_w is assumed to be zero. Also, the surface friction is assumed negligible.

When the end-effector stiffness is adaptively changed by the proposed method in constrained space, the stiffness K_c is replaced as the Eq. (7). Then, the closed-loop dynamics yield

$$\begin{aligned} M(q)\ddot{q} + H(q,\dot{q})\dot{q} &= J^T(q)(K_c(f)\tilde{x} - K_v(f)\dot{x} \\ &\quad -K_w(x - x_w)), \end{aligned} \tag{10}$$

where $\tilde{x}$ is defined as positional tracking error, $x_d - x$, in task space.

To analyze the stability of the system, we utilize the Lyapunov-like function given by

$$\begin{aligned} V &= \frac{1}{2}\dot{q}^T M(q)\dot{q} + \frac{1}{2}\tilde{x}^T K_c(f)\tilde{x} \\ &\quad + \frac{1}{2}(x - x_w)^T K_w(x - x_w). \end{aligned} \tag{11}$$

Differentiating Eq. (11) with respect to time and utilizing Jacobian relationship, $\dot{x} = J(q)\dot{q}$, yield

$$\begin{aligned} \dot{V} &= \frac{1}{2}\dot{q}^T \dot{M}(q)\dot{q} + \dot{q}^T M(q)\ddot{q} \\ &\quad + \frac{1}{2}\tilde{x}^T \dot{K}_c(f)\tilde{x} - \dot{q}^T J^T(q) K_c(f)\tilde{x} \\ &\quad + \dot{q}^T J^T(q) K_w(x - x_w). \end{aligned} \tag{12}$$

Substituting Eq. (10) into Eq. (12) and utilizing Jacobian relationship yield

$$\begin{aligned} \dot{V} &= \dot{q}^T(\frac{1}{2}\dot{M}(q) - H(q,\dot{q}))\dot{q} - \dot{q}^T J^T(q) K_v(f) J(q)\dot{q} \\ &\quad + \frac{1}{2}\tilde{x}^T \dot{K}_c(f)\tilde{x}. \end{aligned} \tag{13}$$

Applying the skew-symmetric property [6] to Eq. (13) and utilizing Eq. (8) yield

$$\dot{V} = -\dot{x}^T \begin{pmatrix} \alpha_x & 0 & 0 \\ 0 & \alpha_y & 0 \\ 0 & 0 & \alpha_z \end{pmatrix} K_c(f)\dot{x} + \frac{1}{2}\tilde{x}^T \dot{K}_c(f)\tilde{x}, \tag{14}$$

where $x = [x_x \ x_y \ x_z]^T$, $\tilde{x} = [\tilde{x}_x \ \tilde{x}_y \ \tilde{x}_z]^T$ in three-dimensional space.

After rearranging Eq. (14), and applying the condition $\dot{V} < 0$, then the following inequality equations are constructed:

$$2\alpha_x \dot{x}_x^2 + \tilde{x}_x^2 s_x \dot{f}_x > 0, \tag{15}$$

$$2\alpha_y \dot{x}_y^2 + \tilde{x}_y^2 s_y \dot{f}_y > 0, \tag{16}$$

and

$$2\alpha_z \dot{x}_z^2 + \tilde{x}_z^2 s_z \dot{f}_z > 0. \tag{17}$$

In Eqs. (15), (16), and (17), the following sufficient conditions for stability can be obtained:

$$0 \le s_x < \frac{2\alpha_x \dot{x}_x^2}{\tilde{x}_x^2 |\dot{f}_x|}, \tag{18}$$

$$0 \le s_y < \frac{2\alpha_y \dot{x}_y^2}{\tilde{x}_y^2 |\dot{f}_y|}, \tag{19}$$

and

$$0 \leq s_z < \frac{2\alpha_z \dot{x}_z^2}{\tilde{x}_z^2 |\dot{f}_z|}. \tag{20}$$

Therefore, for small velocities, and large force variation, α_x, α_y, and α_z are chosen to be sufficiently large in such a way that s_x, s_y, and s_z could be of resonable positive values. In case that each slope is chosen to be zero, the proposed method is the same as the conventional active stiffness control method.

4 Implementation and Experimental Results

4.1 Implementation and Experimental Setup

In Figure 1, the block diagram for the proposed compliance control method is shown. As shown in Figure 1, the task planner gives a surface tracking manipulation task to achieve the following two subgoals simultaneously:

1) minimum variance path following and

2) regulation of a contact force of the axes of the end-effector orthogonal to the position or velocity controlled axes for path following.

The desired quantities of motion are not here specified as fixed functions of time. Instead, they are specified as functions of task-related motion quantities. In addition, a virtual desired path to be followed is intentionally given to be inside the surface of the object of which contact forces are to be regulated. For our experimental system, the task is given as shown in Figure 2. Specifically, the task is given to follow a circle trajectory starting from point A in unconstrained space, to follow the wall in constrained space and to return to point A. The virtual trajectory in our case is given as a part of circle as shown in Figure 2.

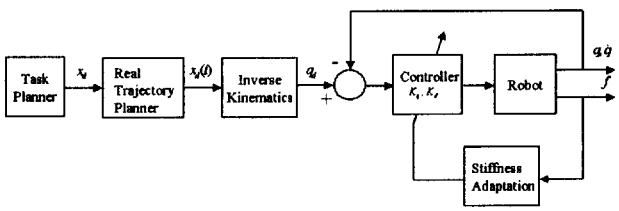

Figure 1: The block diagram for compliant contact control.

For experimental verification of the proposed stiffness control algorithm, our laboratory developed two-link direct drive manipulator is used as shown in Figure 3. The joints are directly actuated by megatorque motors, RS0608FN001 and RS1410FN001 made by Nippon Seiko Ltd. with shaft resolvers which provide motor position measurements. Joint velocities are reconstructed through numerical differentiation of joint position measurements. A six-axis wrist force/torque sensor, Model No. 67M25A-I40 of JR3 Inc., is mounted at the end-effector for measuring contact force/torque. The physical parameters of the manipulator are given in Table 1.

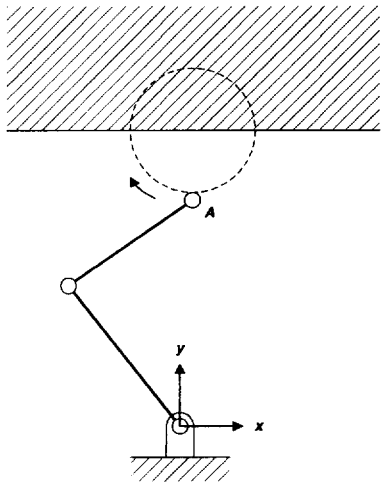

Figure 2: A compliant contact task of two-link manipulator interacting with an unknown environment

Figure 3: Laboratory developed two-link direct drive manipulator and its control system.

Table 1. Physical parameters of the robot manipulator.

Items	*Link* 1	*Link* 2
Length (m)	0.403	0.453
Mass of Link (Kg)	22	12
Mass of motor (Kg)	73	14
Rotor inertia ($Kg_f m^2$)	1.07	0.031

The robot maniplulator is controlled by a VME-bus based real-time control system as shown in Figure 4. The main control loop is working at the in-house DSP-based servo controller. The contact force signal of the end-effector is obtained by force/torque interface board after filtering noise, and then the force information is transmitted into the DSP controller and the single board computer MC68040 through the VME-bus. The analog signals are sampled and digitized by the A/D converter, and the torque commands are transferred to each actuator by the D/A converter. The current joint position of robot manipulator is measured from resolver signal processing units at every sampling time. The control algorithms are coded by a C language. The control signal update and the data feedback for each joint are executed at every 5[msec] with the aids of the real-time O.S. VxWorks [8].

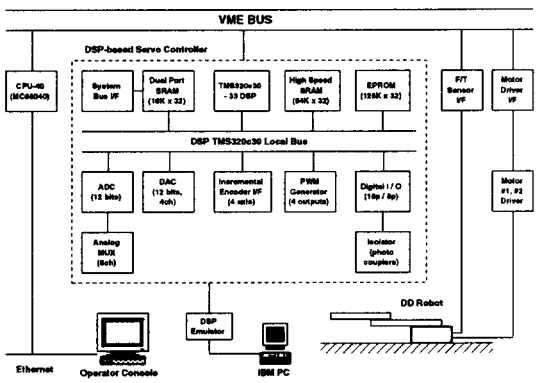

Figure 4: The hardware configuration of the controller for two-link manipulator.

4.2 Experimental Results

To test the effectiveness of the proposed stiffness control algorithm, a simple task is chosen as shown in Figure 2. In the experiments, we give a diameter of circle as 0.15 m and task time to be 10 *secs*.

The experimental results are shown in Figure 5, Figure 6, and Figure 7. For cases of constant stiffness gains of Figure 5, and proposed force error based adaptive stiffness function of Figure 6 and Figure 7, both systems show stable actions throughout all phases of the task. Especially, similar path following performances are obtained. However, the interaction forces in both cases, during the constrained motion phase of the task, are shown to be quite different. From Figure 5, one can observe that if the constant stiffness control is used, an interaction force increases rapidly as a position error and hence the reaction force increases. However, as shown in Figure 6 and Figure 7, interaction forces by the proposed control algorithm become relatively small and moreover, can be reduced more by increasing the slope parameter as shown in Figure 7.

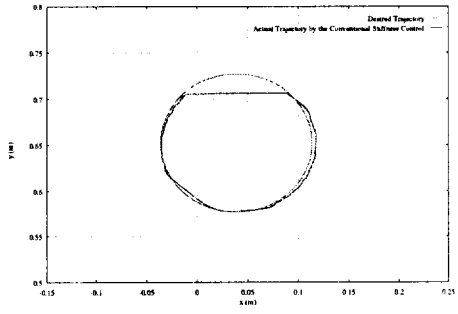

(a) Trajectory of the end-point

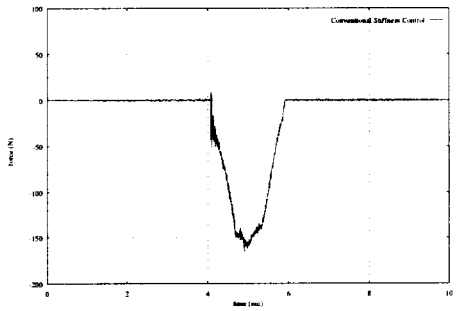

(b) The history of contact force

Figure 5: Actual position and force trajectories in case of when the fixed stiffness gains.

5 Concluding Remarks

A new compliant control strategy was proposed by employing a self-controlled stiffness function for controlling various types of manipulator motions such as path following, initial contact with soft impact and force regulation during contact without both of any switching mechanism in algorithm and any knowledge on the environment in constrained and unconstrained spaces. The proposed method was experimentally

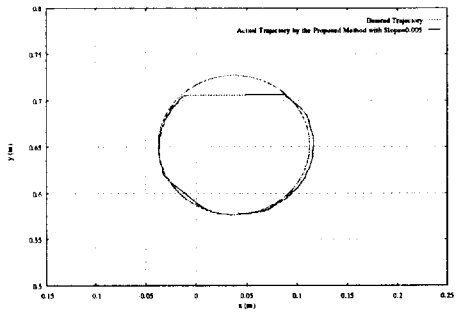

(a) Trajectory of the end-point

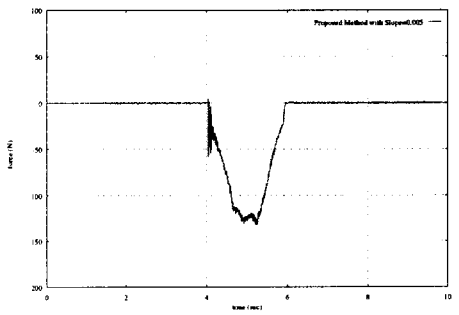

(b) The history of contact force

Figure 6: Actual position and force trajectories when adaptive stiffness law is used($s_x = s_y = 0.005$).

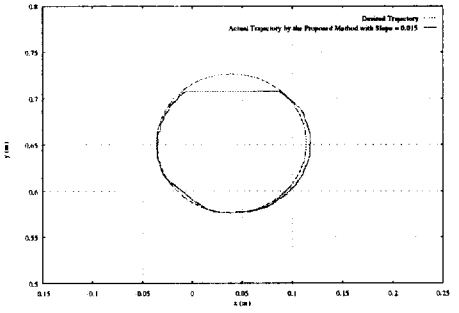

(a) Trajectory of the end-point

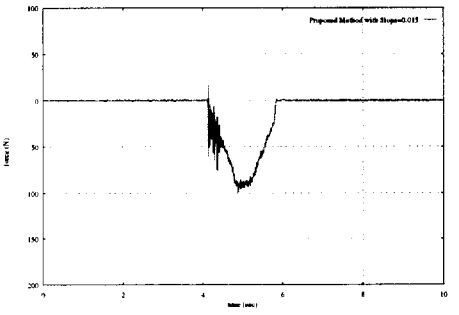

(b) The history of contact force

Figure 7: Actual position and force trajectories when adaptive stiffness law is used($s_x = s_y = 0.015$).

shown to work satisfactorily for a compliance control task by employing laboratory developed two-link manipulator.

References

[1] M. Vukobratović, and A. Tuneski, "Contact Control Concepts in Manipulation Robotics - An Overview," *IEEE Trans. on Industr. Electro.*, Vol, 41, No. 1, pp. 12-24, 1994.

[2] M. H. Raibert and J. J. Craig, "Hybrid Position/Force Control of Manipulators," *ASME J. Dyn. Syst. Meas. Contr.*, Vol. 102, No. 1, pp. 126-133, 1981.

[3] T. Yoshikawa, "Dynamic Hybrid Position/Force Control of Robot Manipulators - Description of Hand Constraints and Calculation of Joint Driving Force," *IEEE J. of Robotics and Automation*, Vol. 33, pp. 386-392, 1987.

[4] S. -R. Oh, H. C. Kim, I. H. Suh, B. -J. You, and C. -W. Lee, "A Compliance Control Strategy for Robot Manipulators Using a Self-Controlled Stiffness Function," *Proc. of IEEE/RSJ Int. Conf. Intelligent Robots and Systems*, Pittsburgh, PA. U.S.A., pp. 179–184, 1995.

[5] S. Chiaverini, B. Sicilliano, and L. Villani, "Force and Position Tracking: Parallel Control With Stiffness Adaptation," *IEEE Control Systems Magazine,* Vol. 18, No. 1, pp. 27-33, 1998.

[6] F. L. Lewis, C. T. Abdallah, and D. M. Dawson, *Control of Robot Manipulators,* Macmillan Publishing Company, 1993.

[7] J. K. Salisbury, "Active Stiffness Control of Manipulator in Cartesian Coordinates," *Proc. of IEEE 19th Conf. on Decision and Control*, pp. 95-100, 1980.

[8] VxWorks Manual, *Real-Time Operating System*, Wind River Systems, 1992.